

Estimation of Partial Discharge Inception Voltage of Magnet Wires under Inverter Surge Voltage by Volume-Time Theory

Naoki Hayakawa

EcoTopia Science Institute

Nagoya University

Furo-cho, Chikusa-ku, Nagoya 464-8603, Japan

Fuminobu Shimizu and Hitoshi Okubo

Department of Electrical Engineering and Computer Science

Nagoya University

Furo-cho, Chikusa-ku, Nagoya 464-8603, Japan

ABSTRACT

This paper discusses a novel estimation method for partial discharge inception voltage (PDIV) of magnet wire under inverter surge voltage application. We focused on the generation probability of initial electrons, which induce PD under high electric field and short rise time of surge voltage, by means of Volume-Time theory. We applied the Volume-Time theory to PD inception phenomena in a wedge-shaped air gap of twisted pair samples composed of enameled wires, and estimated PDIV in consideration of initial electron generation probability with temporal and spatial change in electric field distribution. We could estimate PDIV under different waveforms of applied surge voltage for different specifications of enameled wires. PDIV estimated by the extended Volume-Time theory agreed well with the measured PDIV. The estimated PDIV decreased with the increase in the rise time of applied voltage waveform, which corresponded to the V-t characteristics in the time range of inverter surge voltage.

Index Terms — Inverter surge, Partial discharge (PD), PD inception voltage (PDIV), Initial electron, Discharge generation probability, Volume-Time theory.

1 INTRODUCTION

DEMAND for inverter-fed motors is expanding because of their high efficiency, controllability, environmental value and other advantages. Consequently, both higher power output and efficiency of inverter-fed motors are greatly requested. However, because the inverter surge voltage has a short rise time of nanosecond order, it may cause partial discharge (PD) and degradation of electrical insulation performance of the motor coils [1-7]. Therefore, rational electrical insulation design and evaluation techniques of PD inception voltage (PDIV) for magnet wire of inverter-fed motors are strongly required. In particular, electrical insulation performance against the inverter surge voltage is critical in low-voltage motors for Type I electrical insulation systems [8]. However, the report concerning the estimation of PDIV under surge

voltage condition has not yet been found.

We have been studying the PD inception, insulation degradation and breakdown (BD) characteristics of enameled wires in order to make clear the PD inception phenomena under inverter surge voltage [9-12]. In this paper, we propose a novel estimation method of PDIV based on Volume-Time theory, under inverter surge voltage, from the viewpoint of charge generation and the subsequent charge behavior. Volume-Time theory can compute the generation probability of initial electrons by discussing the temporal and spatial change in electric field distribution. So far, Volume-Time theory has been used for the evaluation of initial electron generation and discharge inception property at bare electrodes under lightning impulse and fast transient voltages in SF₆ gas [13-18]. We computed PDIV by extending the Volume-Time theory to PD inception phenomena in a wedge-shaped air gap of enameled wires under a single shot of inverter surge voltage, and compared it with experimental results.

2 EXPERIMENTAL SETUP

Figure 1 shows the experimental setup. The inverter surge generation circuit consists of dc high voltage supply, high voltage semiconductor switch, pulse generator, coaxial cable (10-50 m) and capacitance (0-2 nF). It can generate negative single surge voltage (damped oscillatory wave), referred to as “Surge”, with rise time $t_r=60-3000$ ns, overshoot ratio (OSR)=150-180 %, defined as the peak/plateau value after oscillation, and pulse width $\tau=10$ μ s. Another negative single surge voltage (non-oscillatory wave), referred to as “Impulse”,

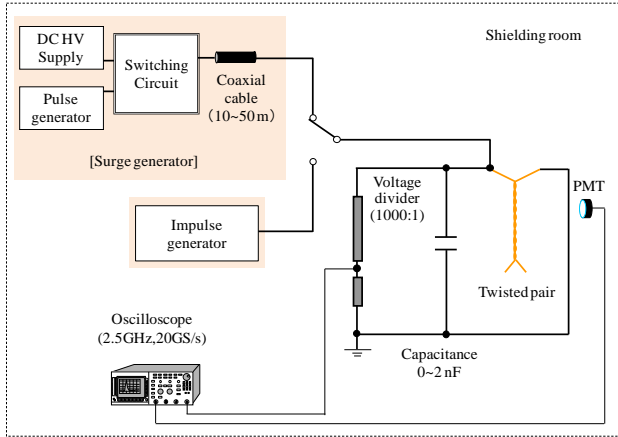


Figure 1. Experimental setup.

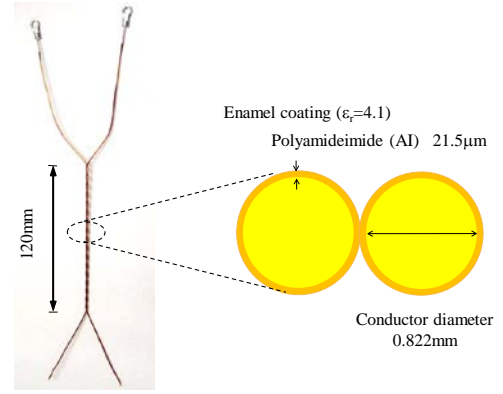


Figure 3. Structure of twisted pair sample (Sample A).

Table 1. Test sample list.

	Conductor diameter [mm]	Enamel coating thickness [μ m]	Material	Dielectric constant	Nano filler rate
Sample A	0.822	21.5	AI	4.1	
Sample B	0.823	10.5	AI	4.1	
Sample C	0.822	30.0	AI	4.1	
Sample D	0.822	34.5	AI	4.1	
Sample E	0.820	41.0	AI	4.1	
Sample F	0.75	20.0	outer: AI inner: EI	3.85	
Sample G	0.75	20.0	outer: AI inner: EI	3.85	1 wt%

AI : polyamideimide EI : polyesterimide

with $t_r=300$ ns and half of pulse width $t_{50\%}=420$ μ s is also generated by another voltage supply. Figure 2 shows 6 waveforms used in this experiment.

In this paper, we used 7 twisted pair samples (A-G) consisted of 2 enameled wires [19] with insulation coating of polyamideimide and polyesterimide. Figure 3 and Table 1 show the structure and specifications of the twisted pair samples. PD signal was detected by PD light intensity with photo multiplier tube (PMT), and PDIV was defined as the value from 0 to peak of the applied surge voltage when PMT has detected PD signal for the first time after the voltage application. The experiment was carried out at a temperature of 20-25 $^{\circ}$ C and a relative humidity of 30-40 %.

3 EXPERIMENTAL RESULTS

PDIV of sample A was measured under single shot of applied voltages with 6 waveforms shown in Figure 2. Figure 4 shows the applied voltage waveform and PD light intensity signal in each case. PD always occurred near the peak of each voltage waveform. PD measurements were repeated 10 times in a fixed condition. Figure 5 shows PDIV for each single shot of applied voltage. PDIV decreased with the increase in the rise time under a fixed pulse width ($\tau=10$ μ s) of Surge I - Surge V, which is consistent with [20] for $t_r<500$ ns. PDIV also decreased with the increase in the pulse width under a fixed rise time ($t_r=300$ ns) of Surge II and Impulse.

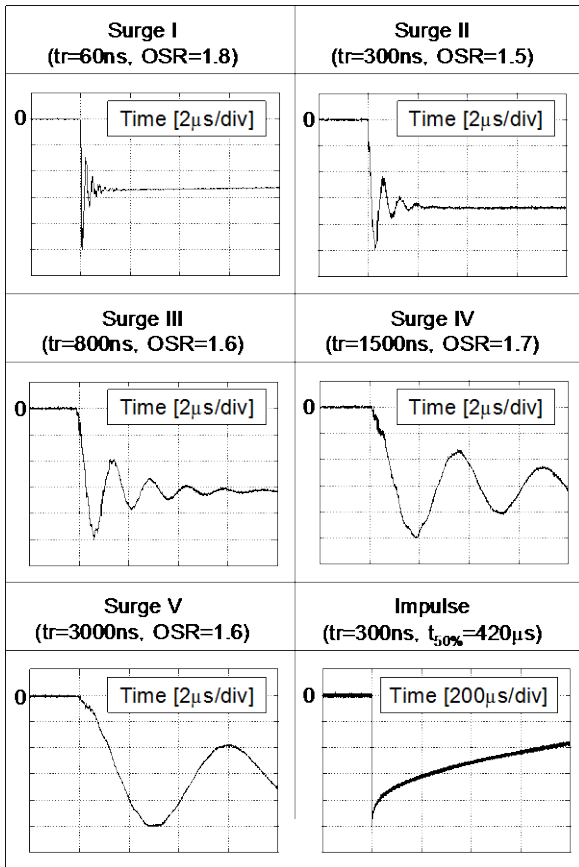


Figure 2. Applied voltage waveforms.

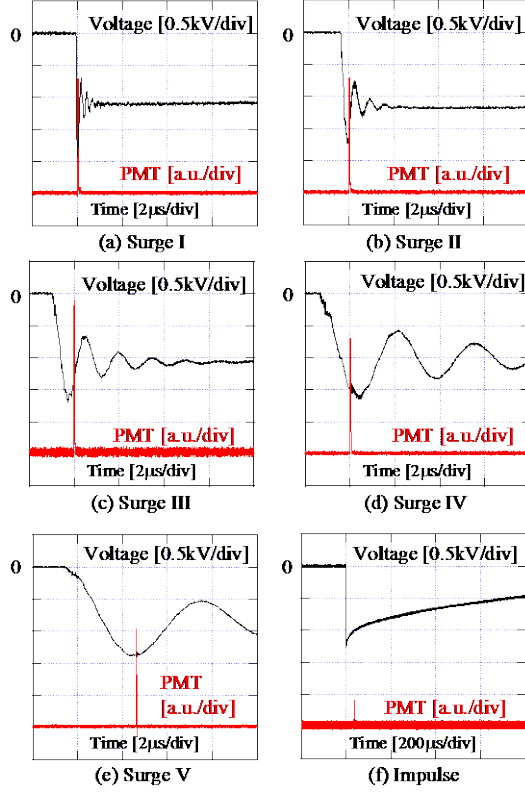


Figure 4. Applied voltage waveforms and PD light intensity signals

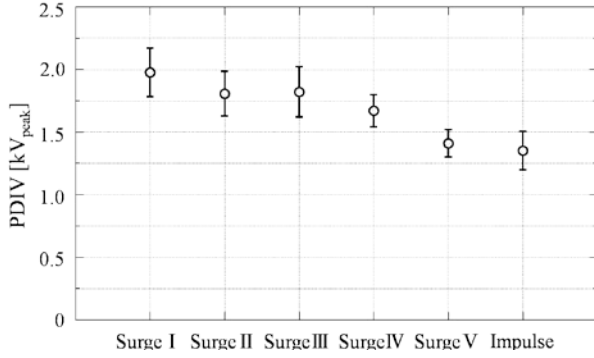


Figure 5. PDIV for different applied voltage waveforms (Sample A).

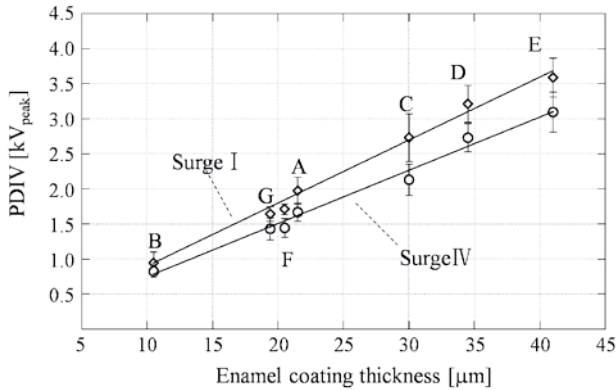


Figure 6. PDIV for different enamel coating thickness (Surge I and IV).

PDIV of 7 twisted pair samples with different enamel coating thickness shown in Table 1 was measured under Surge I and Surge IV shown in Figure 2. Figure 6 shows PDIV as a function of enamel coating thickness. PDIV increased linearly with the increase in the enamel coating thickness.

4 ESTIMATION METHOD OF GENERATION PROBABILITY OF INITIAL ELECTRONS BY EXTENDED VOLUME-TIME THEORY

Volume-Time theory deals with the generation probability of initial electrons in consideration of the temporal and spatial change in electric field distribution, where “Volume” means the volume of high electric field region, and “Time” represents the time stressed by high electric field. Volume-Time theory has been applied to the discharge inception at bare electrodes under lighting impulse voltage in SF₆ gas. In this paper, the Volume-Time theory is extended to the discharge inception at enamel-coated electrodes under inverter-surge voltage in air. The generation probability P of initial electrons is assumed to be computed for an arbitrary voltage waveform by the following equations:

$$P = 1 - \exp \int (V_w + S_w) dt$$

$$V_w = \int_{V_{cr}} \frac{dn_g}{dt} \left(1 - \frac{\eta}{\alpha}\right) dV \quad (1)$$

$$S_w = \int_{S_{cr}} \frac{dn_i}{dt} \left(1 - \frac{\eta}{\alpha}\right) dS$$

where V_w and S_w are defined as the weighted volume and weighted area, respectively, as the frequency [μsec^{-1}] of initial electrons generated in a microscopic area with high electric field per unit time. V_w represents the detached electrons from O_2^- ion in the air gap. S_w represents the electrons from enamel coating and materials attached to enamel surface, which is introduced in this paper as a new parameter to extend the Volume-Time theory. α is electron impact ionization coefficient [mm^{-1}], η is electron attachment coefficient [mm^{-1}] [17], dn_g/dt is the expected value [$\mu\text{sec}^{-1} \text{mm}^{-3}$] of the number of electrons by detachment from O_2^- ion in air gap per unit time and per unit volume, dn_i/dt is the expected value [$\mu\text{sec}^{-1} \text{mm}^{-2}$] of the number of electrons by electronic emission from enamel coating and materials attached to enamel surface per unit time and per unit area. $(1 - \eta/\alpha)$ is the term that represents electrons attached by O_2 molecule in air.

In equation (1), the generation probability of initial electrons is evaluated in the critical Volume V_{cr} [mm^3] in the air gap and critical area S_{cr} [mm^2] on the enamel surface, which can lead to the electron avalanche and PD. V_{cr} and S_{cr} are calculated by the electric field analysis using finite element method, which should also satisfy the following Schuman’s equation for the electron avalanche process:

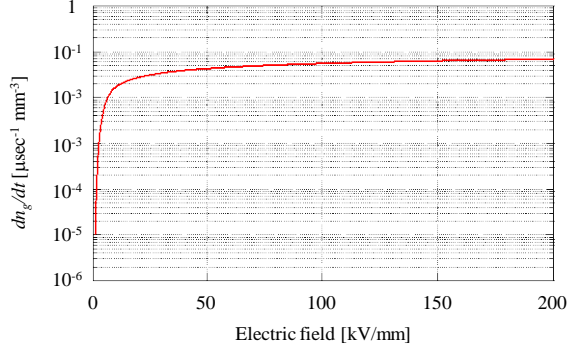


Figure 7. Expected value dn_g/dt of the number of electrons by detachment from O_2^- ion in air gap per unit time and per unit volume as a function of electric field.

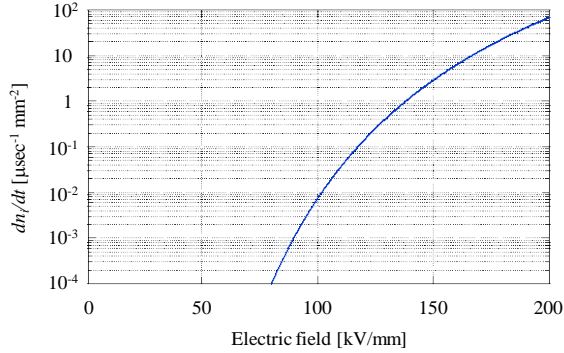


Figure 8. Expected value dn_i/dt of the number of electrons by electronic emission from enamel coating and materials attached enamel surface per unit time and per unit area as a function of electric field.

$$\int_{x_{cr}} (\alpha - \eta) dx = K, \quad (2)$$

where $(\alpha - \eta)$ is effective ionization coefficient, K is constant, x_{cr} shows the distance [mm] along the electric line of force.

dn_g/dt in equation (1) is represented by the following equation:

$$\frac{dn_g}{dt} = k_d \times n^- \quad (3)$$

where n^- is O_2^- density and regarded as a constant, irrespective of time and space. k_d is the expected electron impact ionization frequency and dependent on the electric field strength E [18]. Figure 7 shows dn_g/dt as a function of electric field. With the increase in the electric field, dn_g/dt is saturated, which can not explain the decrease in PDIV under the longer rise time in applied surge voltage waveform in Figure 5.

Then, we introduced dn_i/dt in equation (1) as a new source of initial electrons from solid insulator, i.e. enamel coating and materials attached to enamel surface, to be expressed by

$$\frac{dn_i}{dt} = aE^2 \times \exp\left(-\frac{b}{E}\right) \quad (4)$$

Equation (4) including the parameters a and b is experimentally given, supposing the electron emission under high electric field based on Fowler-Nordheim's equation. Figure 8 shows dn_i/dt as a function of electric field. Even under the high electric field, dn_i/dt sharply increases and can generate initial electrons in the air gap with enamel-coated electrodes.

As shown above, the generation probability of initial electrons leading to electron avalanche in air gap with enamel coating under inverter surge voltage can be computed by the extended Volume-Time theory and Schuman's equation.

5 COMPARISON OF EXPERIMENTAL AND ESTIMATION RESULTS

5.1 CRITICAL VOLUME AND CRITICAL AREA

Figure 9 shows the critical volume V_{cr} and critical area S_{cr} for sample A as a function of instantaneous voltage value. Figure 10 also shows the schematic illustration of V_{cr} and S_{cr} for different applied voltages. In each figure, V_{cr} and S_{cr} increase with the increase in the applied voltage. When an initial electron was generated in V_{cr} or S_{cr} during its existence, the initial electron can grow up to the electron avalanche and PD. In Figure 10, V_{cr} is not symmetric and leans to the cathode (-H.V.) conductor. This is because in order to meet Schuman's equation, it takes relatively long distance for the electrons to drift from the cathode conductor to the ground (GND) conductor under negative high voltage application.

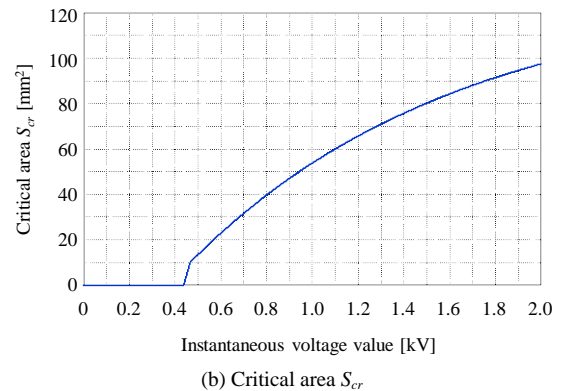
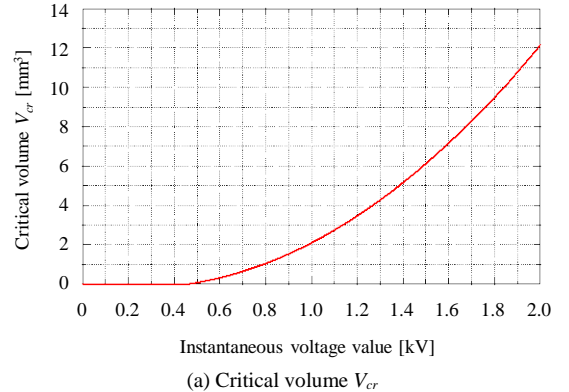
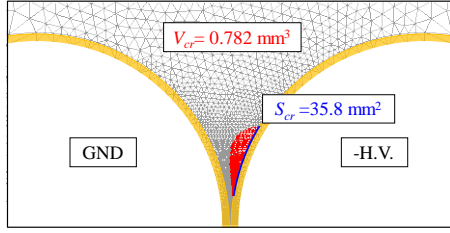
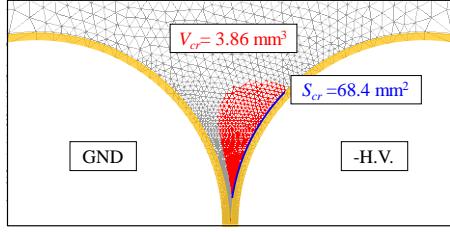


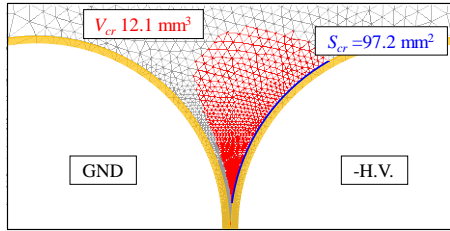
Figure 9. Critical volume V_{cr} and critical area S_{cr} as a function of instantaneous voltage value (Sample A).



(a) Instantaneous voltage value = 0.75kV (ac PDIV)



(b) Instantaneous voltage value = 1.25kV (Impulse PDIV)



(c) Instantaneous voltage value = 2.0kV (Surge I PDIV)

Figure 10. Schematic illustration of critical volume V_{cr} and critical area S_{cr} for different applied voltages (Sample A).

In Figure 10a, V_{cr} and S_{cr} were so small at 0.75 kV corresponding to PDIV under ac voltage, but PD can occur under ac voltage, because the generation probability of initial electrons is quite high even under the slow increase in ac voltage, compared with the behavior of electrons and ions. On the other hand, in Figures 10b and 10c at PDIV under Impulse and Surge I voltages, V_{cr} and S_{cr} become larger with the increase in the applied voltage. The larger V_{cr} and S_{cr} are necessary to generate PD under the applied surge voltage with the shorter rise time.

5.2 PROVIDED INITIAL ELECTRONS

Using the extended Volume-Time theory, PDIV can be discussed by the sum of initial electrons generated in V_{cr} and S_{cr} associated with the temporal change of instantaneous voltage value. Figure 11 shows the relationship between PDIV in Figure 5 and the sum of provided initial electrons based on equation (1) at PDIV for each applied voltage waveform. PDIV decreased with the increase in the sum of provided initial electrons. This means that the sum of provided initial electrons is dominant for PDIV under surge voltage, irrespective of the applied voltage waveform.

Figure 12 shows the weighted volume V_w and weighted area S_w in equation (1) for sample A as a function of instantaneous

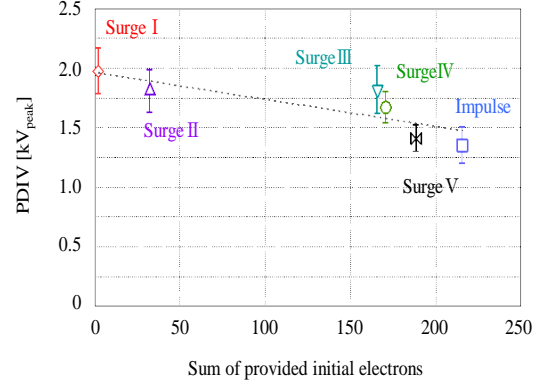


Figure 11. PDIV as a function of sum of initial electrons.

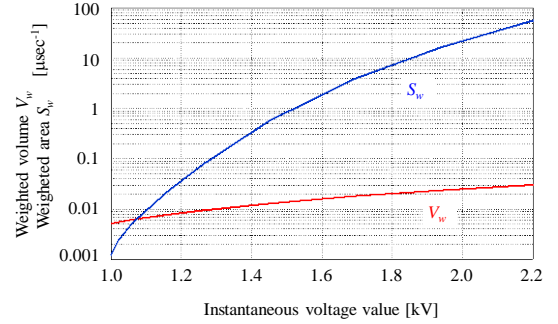


Figure 12. Weighted volume V_w and weighted area S_w (Sample A).

voltage value. Both V_w and S_w increase with the increase in the applied voltage. However, the increase rate of S_w is higher than that in V_w , and the value of S_w is larger than that of V_w at the voltage higher than 1.1 kV. Since PDIV for each sample in Figure 11 was higher than 1.1 kV, S_w can be more decisive than V_w for PDIV. In other words, the initial electrons would be mainly originated from enamel coating and materials attached to enamel surface rather than O_2^- ion in the air gap.

5.3 PDIV UNDER SURGE VOLTAGE

Figure 13 shows the relationship between the computed discharge generation probability and the peak value of applied

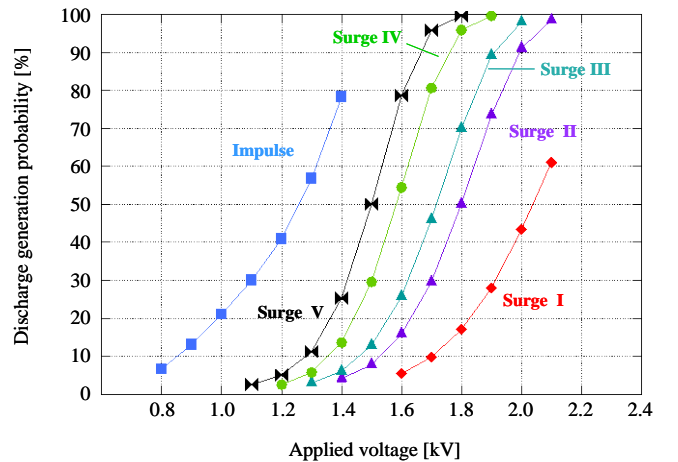


Figure 13. Discharge generation probability as a function of applied voltage (Sample A, Surge I-V and Impulse).

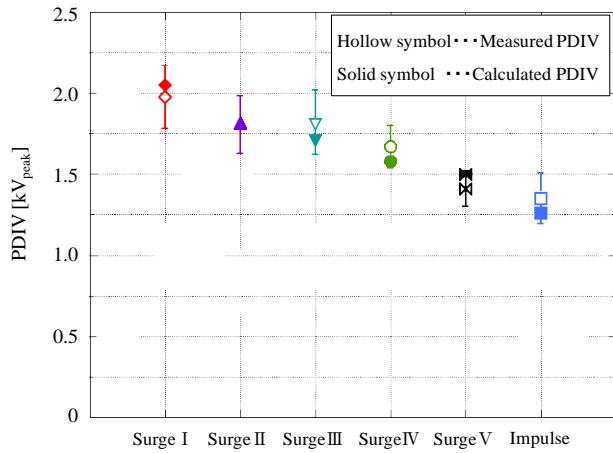


Figure 14. Measured and estimated PDIV for different applied voltage waveforms (Sample A, Surge I-V and Impulse).

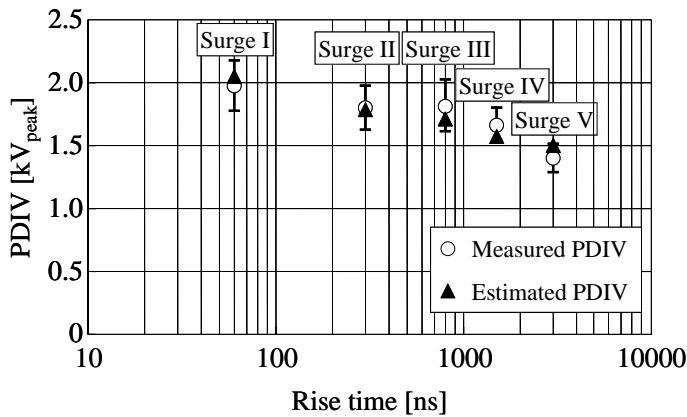
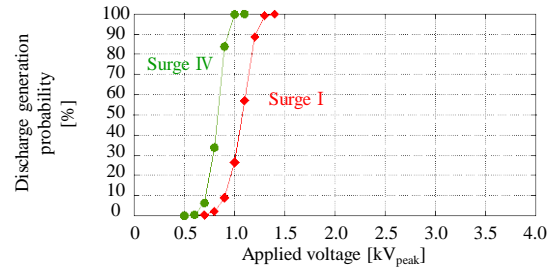


Figure 15. PDIV as a function of rise time of applied surge voltage (Sample A, Surge I-V)

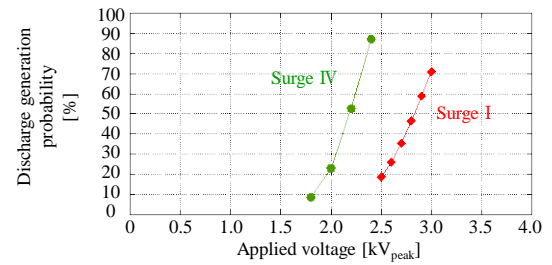
voltage for sample A. The discharge generation probability increases rapidly with the increase in the applied voltage. Here, the estimated PDIV is defined as the value of applied voltage when the discharge generation probability is 50%. Figure 14 shows the estimated PDIV compared with the measured PDIV for sample A in Figure 5. The estimated PDIV agrees well with the measured PDIV in each voltage waveform.

The measured and estimated PDIV are plotted in Figure 15 as a function of rise time of applied surge voltage. PDIV decreased with the increase in the rise time of the applied surge voltage. Such decrease in PDIV against the longer rise time corresponds to the V-t characteristics in the time range of inverter surge voltage for the wedge-shaped air gap with enamel coating.

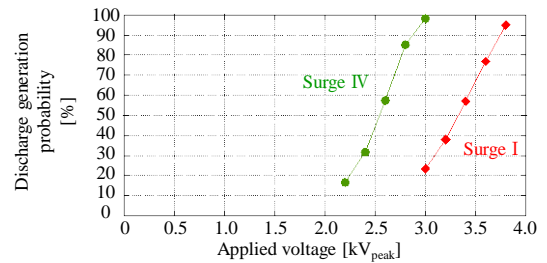
Figures 16a to 16e show the relationship between the computed discharge generation probability and the applied voltage for different samples B - F, respectively. In these figures, \blacklozenge and \bullet show the discharge generation probability under Surge I and Surge IV, respectively. Figure 17 shows the estimated PDIV as a function of enamel coating thickness,



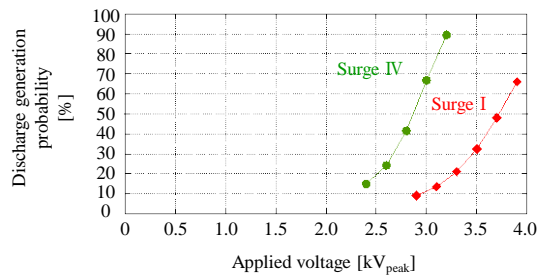
(a) Sample B



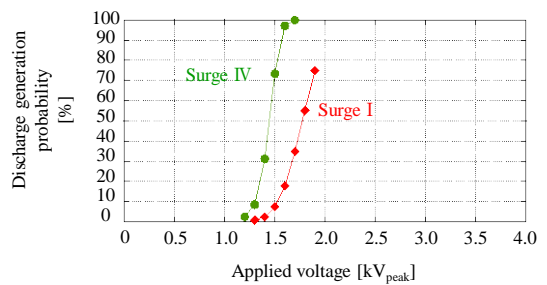
(b) Sample C



(c) Sample D



(d) Sample E



(e) Sample F

Figure 16. Discharge generation probability as a function of applied voltage (Sample B-F, Surge I and IV).

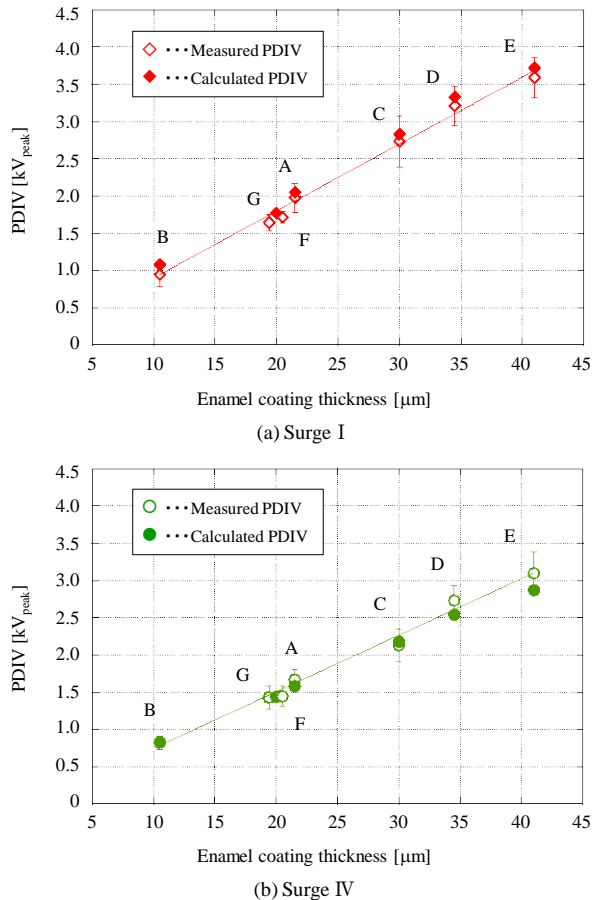


Figure 17. Measured and calculated PDIV for different enamel coating thickness (Sample A-G, Surge I and IV).

together with experimental results in Figure 6. The estimated PDIV rises linearly with the increase in the enamel coating thickness, and agrees well with the experimental results.

Consequently, PDIV in the wedge-shaped air gap under inverter surge voltage can be computed by the extended Volume-Time theory for different waveforms of applied surge voltages and specifications of enameled wires.

6 CONCLUSIONS

In order to establish the estimation method of partial discharge inception voltage (PDIV) under inverter surge voltage, Volume-Time theory was introduced and applied to discharge phenomena in wedge-shaped air gap with enameled wires. PDIV for different kinds of twisted pair samples under different surge voltage waveforms was computed by taking account of generation probability of initial electrons not only in the air gap volume, but also in the surface area of enameled wire. The main results are summarized as follows:

- (1) PDIV under inverter surge voltage could be successfully estimated by the extended Volume-Time theory and Schuman's equation.
- (2) The estimated PDIV was in good agreement with the measured PDIV in each surge voltage waveform and

enameled wire specification, which verified the validity of the proposed method.

- (3) The initial electrons for PD inception would be mainly originated from enamel coating and materials attached to enamel surface rather than O_2^- ion in the air gap.
- (4) According to the estimation of PDIV by the proposed method, PDIV decreased for the applied voltage waveform with the longer rise time, which corresponded to the V-t characteristics in the time range of inverter surge voltage.

REFERENCES

- [1] IEC62068-2: Electrical insulation systems – Electrical stresses produced by repetitive impulses – Part 2: State of the art, 2001.
- [2] M. Kaufhold, G. Borner, M. Eberhardt and J. Speck, "Failure Mechanism of Low Voltage Electric Machines Fed by Pulse-Controlled Inverters", *IEEE Electr. Insul. Mag.*, Vol.12, No.5, pp.9-15, 1996.
- [3] G. C. Stone, S. R. Campbell and S. Tetreault, "Inverter-fed Drives: Which Motor Stators Are at Risk?", *IEEE Industry Appl. Mag.*, Vol. 6, No.5, pp.17-22, 2000.
- [4] J. C. G. Wheeler, "Effects of Converter Pulses on the Electrical Insulation in Low and Medium Voltage Motors", *IEEE Electr. Insul. Mag.*, Vol. 21, No.2, pp. 22-29, 2005.
- [5] K. Kimura, S. Ushirone, T. Koyanagi and M. Hikita, "PDIV characteristics of twisted-pair of magnet wires with repetitive impulse voltage", *IEEE Trans. Dielectr. Electr. Insul.*, Vol.14, pp.744-750, 2007.
- [6] H. Okubo, N. Hayakawa and G. C. Montanari, "Technical Development on Partial Discharge Measurement and Electrical Insulation Techniques for Low Voltage Motors Driven by Voltage Inverters", *IEEE Trans. Dielectr. Electr. Insul.*, Vol. 14, pp.1516-1530, 2007.
- [7] T. Takino, Y. Murakami, N. Hozumi and M. Nagao, "Evaluation of Partial Discharge under Inverter Surge Application Using Current Waveform", *IEEE Conf. Electr. Insul. Dielectr. Phenomena (CEIDP)*, Paper No. 5B-7, 2010.
- [8] IEC60034-18-41TS Ed.1: Rotating electrical machines Part 18-41: Qualification and type tests for Type I electrical insulation systems used in rotating electrical machines fed from voltage converters, 2006.
- [9] N. Hayakawa and H. Okubo: "Partial discharge characteristics of inverter-fed motor coil samples under ac and surge voltage conditions", *IEEE Electr. Insul. Mag.*, Vol.21, No.1, pp.5-10, 2005.
- [10] N. Hayakawa, M. Morikawa and H. Okubo, "Partial Discharge Inception and Propagation Characteristics of Magnet Wire for Inverter-Fed Motor under Surge Voltage Condition", *IEEE Trans. Dielectr. Electr. Insul.*, Vol.14, pp. 39-45, 2007.
- [11] N. Hayakawa, H. Inano, Y. Nakamura and H. Okubo, "Time Variation of Partial Discharge Activity Leading to Breakdown of Magnet Wire under Repetitive Surge Voltage Application", *IEEE Trans. Dielectr. Electr. Insul.*, Vol. 15, pp.1701-1706, 2008.
- [12] N. Hayakawa and H. Okubo, "Lifetime Characteristics of Nanocomposite Enameled Wire under Surge Voltage Application", *IEEE Electr. Insul. Mag.*, Vol. 24, No. 2, pp. 22-27, 2008.
- [13] D. Kind, "Die Aufbaufläche bei Stoss-Spannungsbeanspruchung, technischer Elektroanordnungen in Luft", *Elektronische Zeitschrift Ausgabe A (ETZ-A)*, Vol. 79, pp. 65-69, 1958.
- [14] W. Boeck, "Volumen-Zeit-Gesetz beim Stossspannungsdurchschlag von SF₆", *Elektronische Zeitschrift Ausgabe A (ETZ-A)*, Vol. 96, pp. 300-305, 1975.
- [15] W. Knorr, "A Model to Describe The Ignition Time-Lag of Slightly Nonuniform Arrangements in SF₆", 3rd Int'l. Sympos. High Voltage Engineering (ISH), No.31.11, 1979.
- [16] N. Wiegart, L. Niemyer, F. Pinnekamp, W. Boeck, J. Kindersberger, R. Morrow, W. Zaengl, M. Zwicky, I. Gallimberti and S. A. Boggs, "Inhomogeneous Field Breakdown in GIS - The Prediction of Breakdown in SF₆", *IEEE Trans. Power Delivery*, Vol. 3, pp. 923-930, 1998.

- [17] X. Xu, S. Jayaram and S. A. Boggs, "Prediction of Breakdown in SF₆ under Impulse Conditions", IEEE Trans. Dielectr. Electr. Insul., Vol. 3, pp. 836-842, 1996.
- [18] H. Okubo, H. Shumiya, M. Ito, K. Kato, "Insulation Performance of Permittivity Graded FGM (Functionally Graded Materials) in SF₆ Gas under Lightning Impulse Conditions", IEEE Int'l. Sympos. Electr. Insul., pp.332-335, 2006.
- [19] IEC60851-5: Winding wires - Test methods - Part 5: Electrical properties, 2008.
- [20] M. Fenger, G.C. Stone and B.A. Lloyd "The Impact of Humidity on PD Inception Voltage as a Function of Rise-Time in Random Wound Motors of Different Design", IEEE Conf. Electr. Insul. Dielectr. Phenomena (CEIDP), pp. 501-505, 2002.
- [21] M. N. Swamy and J. A. Harrison, "Effect of attachment and multiple ionization on $\ln(\alpha/p)$ against p/E curves", J. Appl. Phys. J. Phys. D, Vol. 2, pp. 2049-2059, 1969
- [22] D. W. Goodson, R. J. Corbin, L. Trommhold: "Electron avalanches in oxygen: Detachment from the diatomic ion O₂⁺", Phys. Rev, Vol. A9, pp. 2049-2059, 1974.



Naoki Hayakawa (M'90) was born on 9 September 1962. He received the Ph.D. degree in 1991 in electrical engineering from Nagoya University. Since 1990, he has been at Nagoya University and presently he is a Professor of Nagoya University at the EcoTopia Science Institute. From 2001 to 2002, he was a guest scientist at the Forschungszentrum Karlsruhe, Germany. He is a member of IEE of Japan and CIGRE.



Fuminobu Shimizu was born on 11 September 1985. He received the M.S. degree in 2010 in electrical engineering from Nagoya University, and joined Chubu Electric Power Co., Inc.



Hitoshi Okubo (M'81) was born on 29 October 1948. He received the Ph.D. degree in 1984 in electrical engineering from Nagoya University. He joined Toshiba Corporation, Japan in 1973 and was a Manager of HV laboratory of Toshiba. From 1976 to 1978, he was at the RWTH Aachen, Germany and the TU Munich, Germany. In 1989 he became an Associate Professor and presently he is a Professor of Nagoya University in the Department of Electrical Engineering and Computer Science. He is a member of IEE of Japan, VDE and CIGRE.